

Supplementing Materials for, “Estimating Under Five Mortality in Space and Time in a Developing World Context”

Journal Title
XX(X):1–27
© The Author(s) 2017
Reprints and permission:
sagepub.co.uk/journalsPermissions.nav
DOI: 10.1177/ToBeAssigned
www.sagepub.com/


Jon Wakefield^{1,2}, Geir-Arne Fuglstad³, Andrea Riebler³, Jessica Godwin¹,
Katie Wilson² and Samuel J. Clark⁴

1 HIV Adjustment

Suppose we have m months with monthly hazards ${}_1q_i$, $i = 0, \dots, m$. We have,

$$\text{Survival} = \prod_{i=1}^m (1 - {}_1q_i).$$

Taking logs:

$$\log(\text{Survival}) = \sum_{i=0}^m \log(1 - {}_1q_i) \approx - \sum_{i=1}^m {}_1q_i$$

So

$$\text{Survival} = \exp \left(- \sum_{i=0}^m {}_1q_i \right)$$

and

$$\text{Death} = {}_5q_0 = 1 - \exp \left(- \sum_{i=0}^m {}_1q_i \right) \approx 1 - \left[1 - \sum_{i=0}^m {}_1q_i \right] = \sum_{i=0}^m {}_1q_i.$$

¹Department of Statistics, University of Washington, Seattle

²Department of Biostatistics, University of Washington, Seattle

³Department of Mathematical Sciences, Norwegian University of Science and Technology, Trondheim

⁴Department of Sociology, The Ohio State University, Columbus

Email: jonno@uw.edu

So if we have a multiplicative bias on all the hazards this will result (approximately) in the same multiplicative bias on the U5MR. The approximation is more accurate if the hazards are small. We now show how we can add an offset to the logistic regression model on the hazard, in order to adjust for bias.

Let ${}_5q_0$ be true U5MR and ${}_5\widetilde{q}_0$ the biased (unadjusted for HIV) U5MR in a generic survey and year. We have an estimate of

$$\text{BIAS} = \frac{{}_5q_0}{{}_5\widetilde{q}_0} \geq 1.$$

We assume the bias acts the same on all age groups and model it through an offset for each hazard,

$$\log\left(\frac{{}_1q_i}{1 - {}_1q_i}\right) = \log\left(\frac{{}_1\widetilde{q}_i}{1 - {}_1\widetilde{q}_i}\right) + \log(\text{BIAS}),$$

where ${}_1q_i$ and ${}_1\widetilde{q}_i$, are the corrected and uncorrected hazards, respectively for month $i = 1, 2, \dots, 60$. Under the assumption that each hazard is small, each logit is also small and

$${}_1q_i = \frac{\exp[\text{logit}({}_1\widetilde{q}_i) + \log(\text{BIAS})]}{1 + \exp[\text{logit}({}_1\widetilde{q}_i) + \log(\text{BIAS})]} \approx \exp[\text{logit}({}_1\widetilde{q}_i)] \times \text{BIAS} \approx {}_1\widetilde{q}_i \times \text{BIAS},$$

which means that the bias is acting the same on each hazard. Hence,

$${}_5q_0 \approx \sum_{i=1}^m {}_1q_i \approx \text{BIAS} \times \sum_{i=1}^m {}_1\widetilde{q}_i \approx \text{BIAS} \times {}_5\widetilde{q}_0,$$

and the log-offset in the logits for the hazards approximatively give a multiplicative bias correction of the U5MR.

2 Constructing a Space-Time Surface

Figure 1 shows the posterior median estimates of U5MR and Figure 2 the corresponding standard deviation. As indicated in Figure 8 of the main text, it can be seen that the drop in the central region of Kenya is not as large as in the other regions, whereby the U5MR estimates in 1980 are also smaller compared to the non-central areas. The map of 2020 looks very flat. However, we would like to emphasize that the color scale is misleading. The U5MR values are by no means negligible and the corresponding uncertainty is also high, as seen in Figure 2. This is also clearly indicated in the county level plot of the main text.

Figure 3 shows maps of the posterior standard deviation for the spatio-temporal odds. The uncertainty seems to decrease over time and increases again for the extrapolation to 2020. The uncertainty in the central regions seems to be always smaller but looking at Figure 7 of the main text it can be seen that also the estimates are much smaller.

Computing the weighted (directe) estimates involves fitting a separate GLM model (adjusting for the survey design) for each combination of the 47 administrative regions and the seven periods of interest. In this way it is not possible to borrow strength from the other time periods or regions. Figure 4 shows that this leads to a much larger uncertainty in the direct estimates compared to our model estimates. While we believe that our uncertainty estimates might be a little too narrow, the uncertainty of the direct estimates seems very large. Regarding the point estimates, it can be seen that for the early periods the

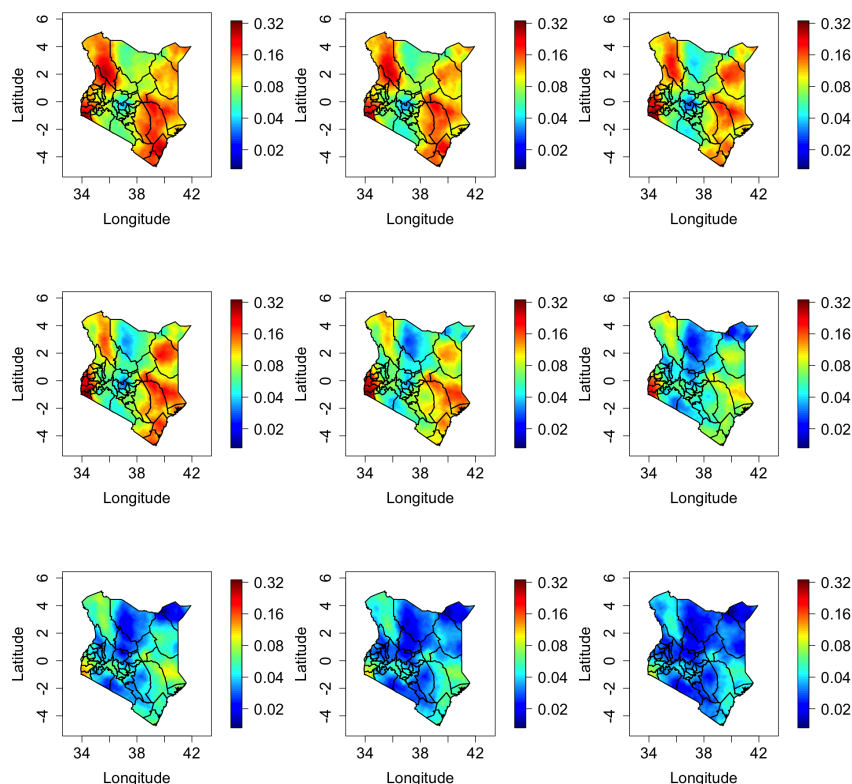


Figure 1. Maps of the posterior median estimates of U5MR Top row: 1980, 1985, 1990. Middle row: 1995, 2000, 2005. Bottom row: 2010, 2015, 2020..

model estimates are much smaller for counties where the direct estimates are large. This phenomenon slightly disappears over time. However, the model estimates seem to get larger for counties where the direct estimates are small.

Evaluation of the spatio-temporal model was done by splitting the clusters in DHS2014 randomly into 397 clusters for training data and 1,187 clusters for testing data. The random splitting always has 1/4 of the clusters of each stratum in the training data and 3/4 of the clusters in the test data when possible. When this split is not possible the remaining clusters are divided randomly between the training data and the test data, but the training data receives at most one of the additional clusters. The spatio-temporal model was then fitted to the training data to produce model estimates of U5MR for each county for each 5-year time period and the method of direct estimates were applied to produce direct estimates of U5MR for each county and for each 5-year time period. These are then compared to the “true” U5MR obtained by direct estimates from the test data for each county and period. Figure 5 shows that the model estimates

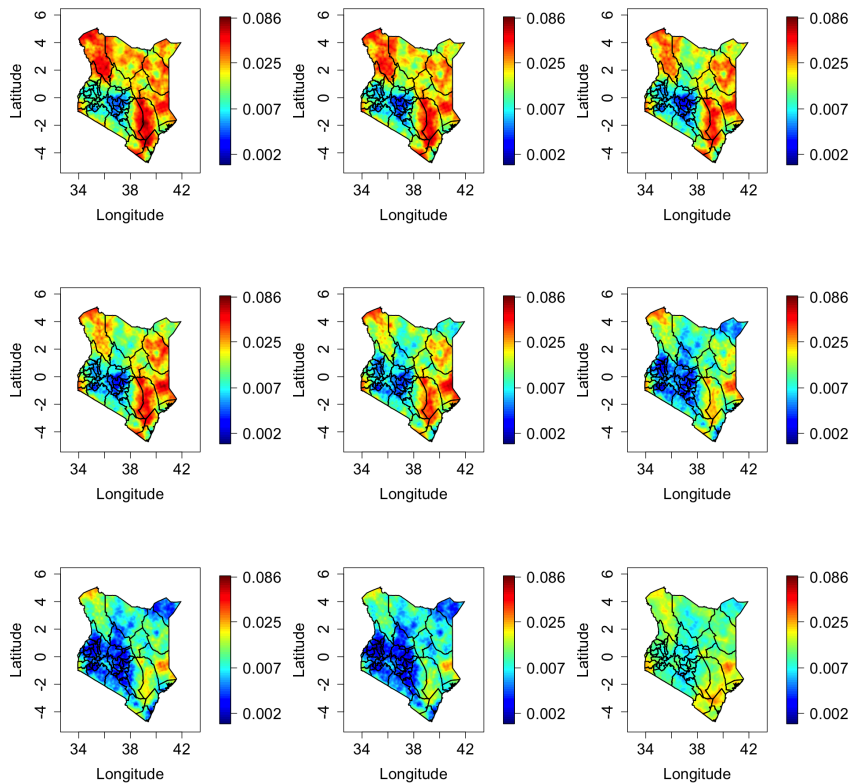


Figure 2. Maps of the posterior standard deviation estimates of U5MR Top row: 1980, 1985, 1990. Middle row: 1995, 2000, 2005. Bottom row: 2010, 2015, 2020.

from the spatio-temporal model has less variation from the true values than the direct estimates and that overall the spatio-temporal model performs better than the method of direct estimation for this test data.

The estimated baseline age-specific components of the logit of the hazard of each age groups is given by an intercept and a temporal second-order random walk. The remaining components of the spatio-temporal model are shared between the age groups and shift the pattern of the logit of the hazards, but cannot change the pattern. Figure 6 shows how the estimated age-specific components of the discrete hazard functions for under-five children in Kenya changes over time. The hazards of each age group has changed with time, but the overall pattern of decreasing mortality over the age groups remains the same.

The national trend found by aggregating the pixel level predictions up to national level is shown in Figure 7. The figure shows that the estimates are close to the B3 model (Alkema et al. 2014; Alkema and New 2014) for earlier time periods, but that for later time periods the estimates are consistently lower. This is expected as the B3 model also incorporates datasets with summary birth histories, which suggest higher values in the later time periods than in the DHS datasets that we analyze. The national estimates

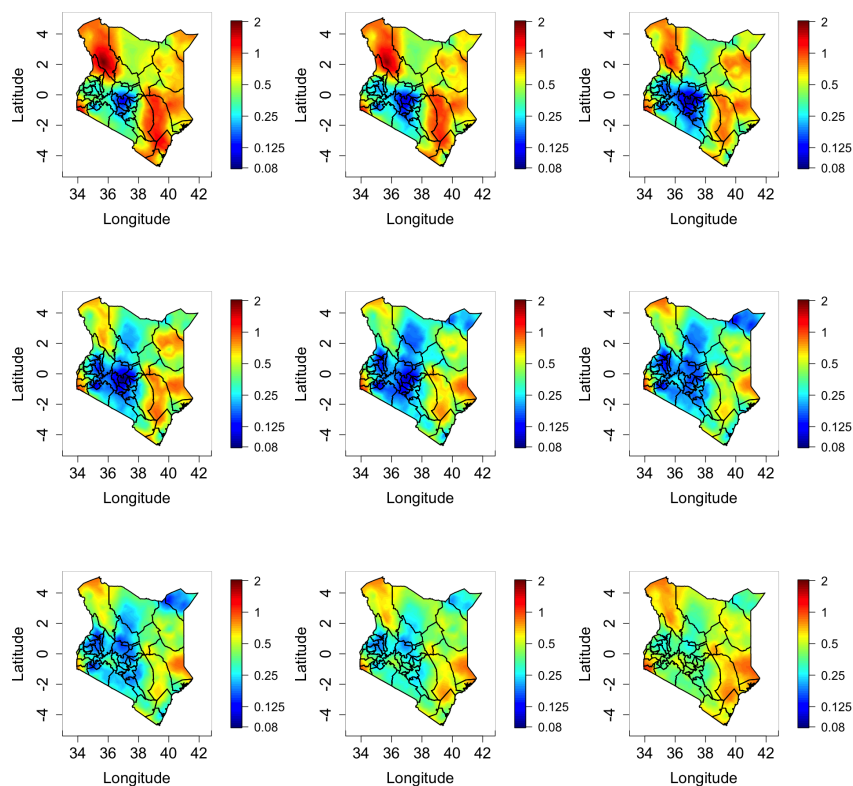


Figure 3. Maps of the posterior standard deviation for the spatio-temporal odds surface, $\exp[u(s, t)]$. Top row: 1980, 1985, 1990. Middle row: 1995, 2000, 2005. Bottom row: 2010, 2015, 2020. Top row: 1980, 1985, 1990. Middle row: 1995, 2000, 2005. Bottom row: 2010, 2015, 2020.

from the spatio-temporal model fit well with the the direct estimates of national U5MR from the different DHS.

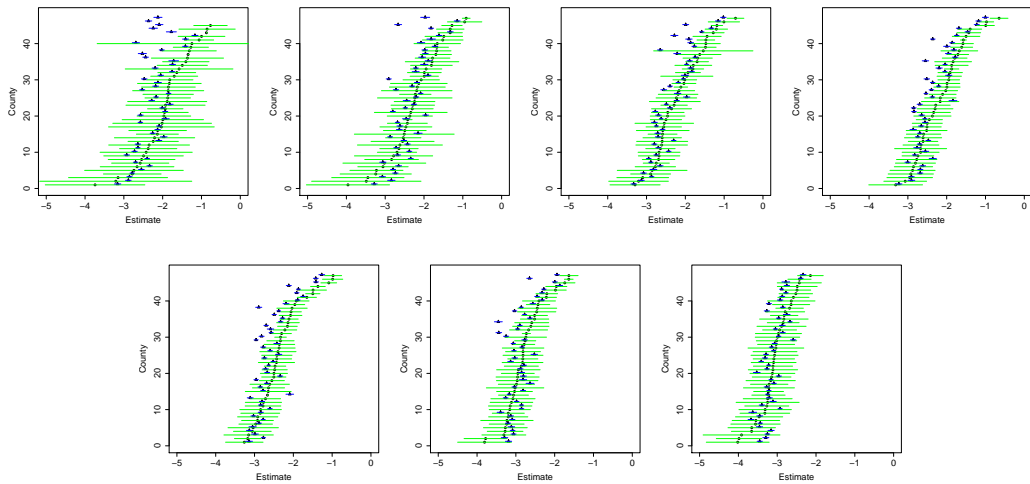


Figure 4. Comparison of our model estimates (green) versus direct estimates (blue) on the logit scale for all seven time periods. For both approaches 95% credible or confidence intervals are provided. Top row: 1980–1984, 1985–1989, 1990–1994, 1995–1999. Bottom row: 2000–2004, 2005–2009, 2010–2014.

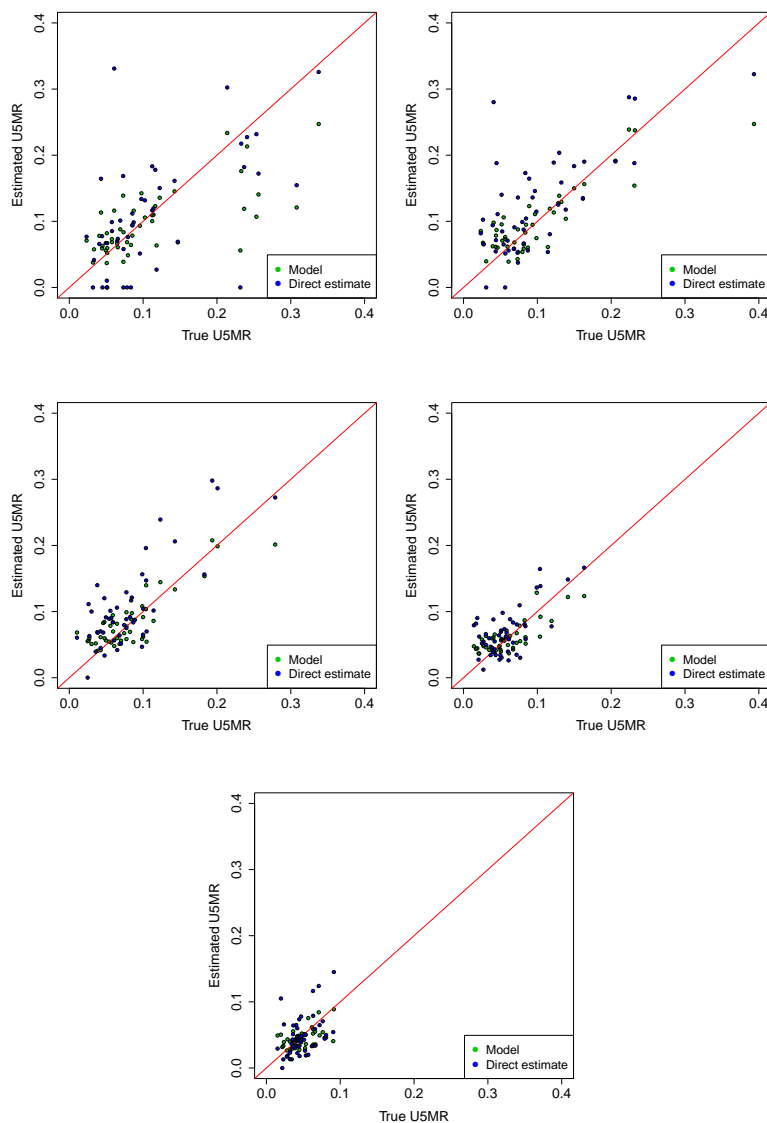


Figure 5. The “true” values obtained by direct estimates from the approximately 1200 hold-out clusters in DHS2014 plotted against the model estimates (in green) and direct estimates (in blue) using data from DHS2003, DHS2008/09 and the (approximately) 400 training clusters in DHS2014. From top left to bottom center the figures are the comparisons for the time periods 1990–1994, 1995–1999, 2000–2004, 2005–2010 and 2010–2014.

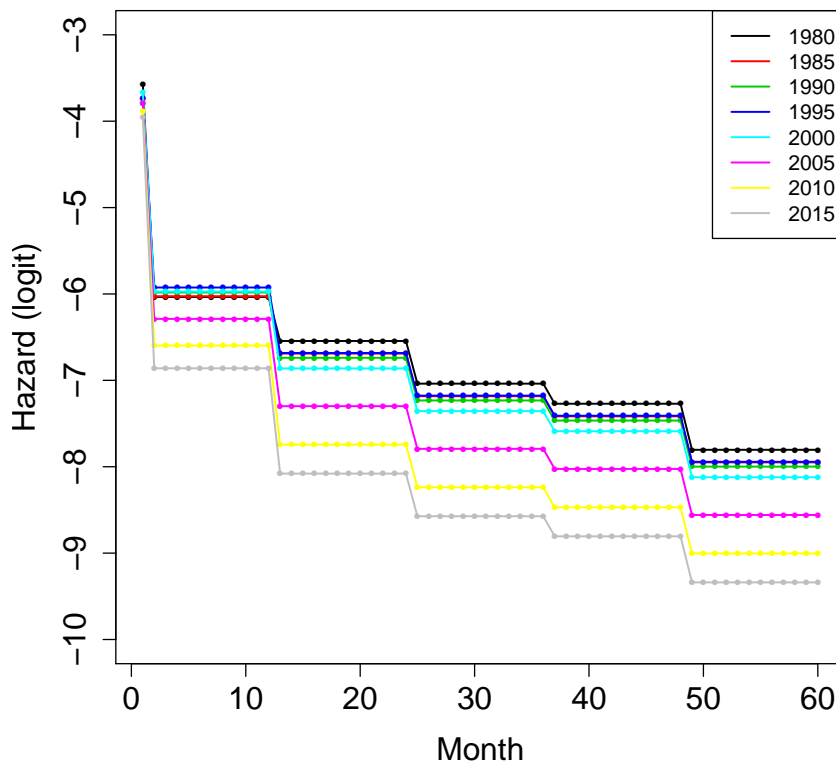


Figure 6. The estimated mean of the age-group-specific baseline of the logit of the discrete hazard function for different years. This includes age-specific intercepts and second-order random walks.

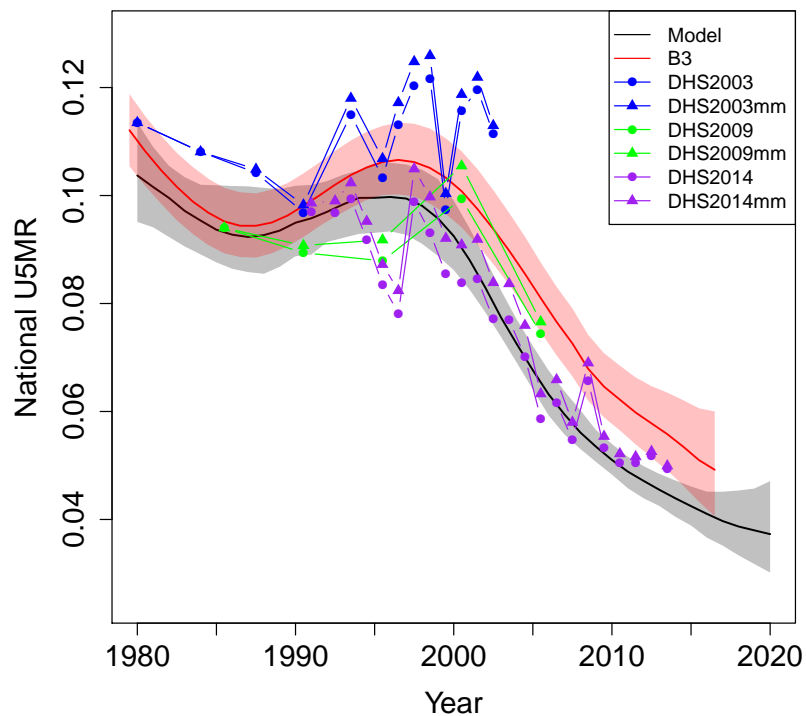


Figure 7. National estimates from DHS2014, DHS2009 and DHS2003 with and without HIV adjustment are compared to our model estimates with 95% CI envelope and to the UNICEF estimates based on the B3 model. The DHS with “mm” in the labels contain an adjustment for maternal mortality.

3 Exploratory Covariate Modeling

The wealth index is a composite measure of many household indicators, and provides information on household socioeconomic status, which is thought to be associated with health. Wealth indices were computed for each household and survey using a set of variables that are commonly available across different DHS. These wealth indices were then compared to the standard DHS wealth index (Rutstein and Johnson 2004; Rutstein 2015) and found to be in good alignment. We used the derived version as the basis for our modeling of the wealth index surface. We obtain a spatially-varying wealth index by modeling the average wealth index at each cluster.

Let $y_k(s_j)$ be the average household wealth index at cluster location s_j in DHS k ($k = 1, 2, 3$) and $N(s_j)$ be the number of households surveyed. We assume the model,

$$y_s(s_j) \mid \beta_0, S_s(s_j), \sigma_k^2, N(s_j) \sim N\left(\beta_0 + S(s_j), \frac{\sigma_k^2}{N(s_j)}\right),$$

where $S(s_j)$ is a spatial random effect with variance λ^2 and range ϕ . We take as the spatial model a GRF with Matérn covariance function, and use the SPDE method (Lindgren et al. 2011) to approximate the field and fit the model. The resultant parameter estimates are in Table 1; we used the predicted mean average household wealth index for each of the three DHS as the covariate surface.

Parameter	2003 Survey	2008 Survey	2014 Survey
β_0	-1.33 (-1.89, -0.880)	-1.17 (-1.76, -0.68)	-1.11 (-1.44, -0.81)
σ^2	45.8 (39.2, 53.6)	47.4 (39.9, 56.4)	31.9 (29.3, 34.7)
λ^2	1.48 (0.977, 2.25)	2.27 (1.52, 3.41)	2.23 (1.81, 2.75)
ϕ	0.632 (0.360, 1.06)	0.705 (0.416, 1.16)	0.48 (0.374, 0.621)

Table 1. Parameter estimates (posterior medians) and 95% credible intervals (CIs) for the wealth index surface model.

A description of the eight spatial covariates we considered in our model is provided in Table 2. Density plots of the eight variables are presented in Figure 8. We note that there is not perfect alignment between the frequency of the spatial covariates at the cluster locations and the overall distribution over Kenya. This is not surprising given that the cluster locations are not uniformly dispersed.

We would like to take an exploratory associations between the logit of U5MR and the covariates. Since we are modeling at the point level, we would like to obtain logit U5MR estimates at points, but unfortunately these are rarely available from the raw data due to the sparsity of deaths. Hence, we obtain the predicted logit U5MR using the model described in Section 3.1 of the paper. These predictions are then plotted against the values of the covariates at grid locations throughout Kenya in Figure 9. We see that *PfPR* appears to have the strongest (positive) association with U5MR. Since many clusters in Kenya are located in areas that are *Pf* free, we opted to break *PfPR* into two components. We included an indicator term for *Pf* free and a second term of log transformed *PfPR* (this term was 0 for areas/clusters that are *Pf* free).

As described in the paper, we divided the clusters into training and test datasets; the locations of these clusters is in Figure 10. We fit the covariate models on the training set and assess model performance using the DIC, WAIC, and CPO criteria. These values are shown in Figures 11 and 12 for models M_3

Variable	Years	Resolution	Source
Access: travel time in minutes to nearest city of 50,000 or more	2000	30 arc seconds	Joint Research Centre of the European Commission http://forobs.jrc.ec.europa.eu/products/gam/download.php
Aridity: function of precipitation availability and atmospheric water demand	Mean value over period 1950-2000	30 arc seconds	CGIAR-CSI http://www.cgiar-csi.org/data/global-aridity-and-pet-database
Temperature: average daily temperature in °C	Mean value over period 1970-2000	30 arc seconds	WorldClim http://worldclim.org/version2
Precipitation: total annual precipitation in mm	Mean value over period 1970-2000	30 arc seconds	WorldClim http://worldclim.org/version2
PfPR: Percent of 2-10 year olds infected by <i>Plasmodium falciparum</i> parasite per year	2000-2014	150 arc seconds	Malaria Atlas Project http://www.map.ox.ac.uk/
Vegetation: Enhanced vegetation index	2000-2014	1km	NASA EOSDIS Land Processes DAAC https://lpdaac.usgs.gov/dataset_discovery/modis/modis_products_table/mod13a3_v006
Population	2000-2014	5km	WorldPop http://www.worldpop.org.uk/data/get_data/
Wealth Index: modeled wealth scores based on the DHS wealth index	2003, 2008, 2014	NA	NA

Table 2. Potential covariates to be used in our model.

and M_4 , respectively. As can be seen in these figures there is good agreement across all measures, with models having lower scores being favorable. Both M_3 and M_4 include *PfPR*; M_3 also includes a term for temperature and M_4 a term for precipitation.

We also compared the relationship between *PfPR* and the other two selected variables: temperature (Figure 13) and precipitation (Figure 14). They are not particularly strongly related.

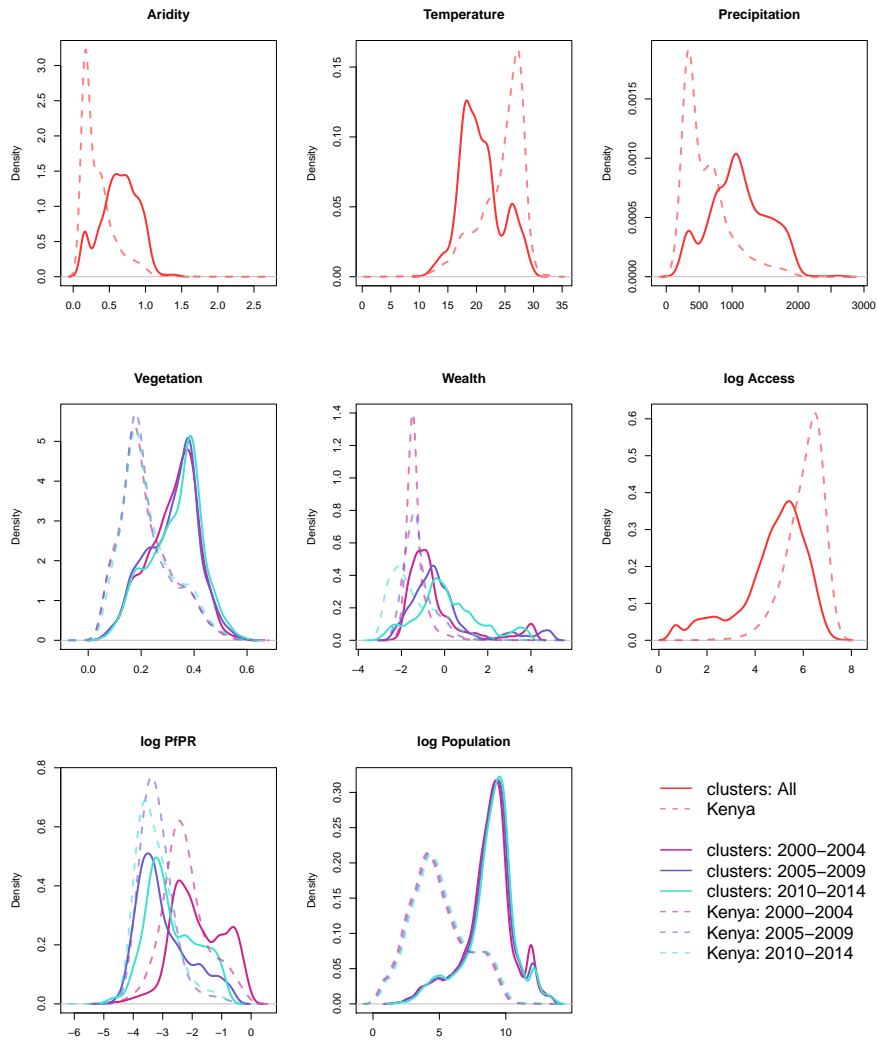


Figure 8. Density plots of the covariates. Access, population, and *PfPR* were transformed to the log scale. Solid lines indicate density of the covariates at the cluster locations. Dashed lines indicate the density of the covariates evaluated on a grid over Kenya.

The posterior median and standard deviation of the predicted U5MR surface for models M_2 , M_3 , and M_4 is shown in Figures 15 and 17, respectively. Corresponding versions on the log scale are provided in Figure 16 and 18. Models M_2 and M_4 have the most visible similarities, and have a larger posterior

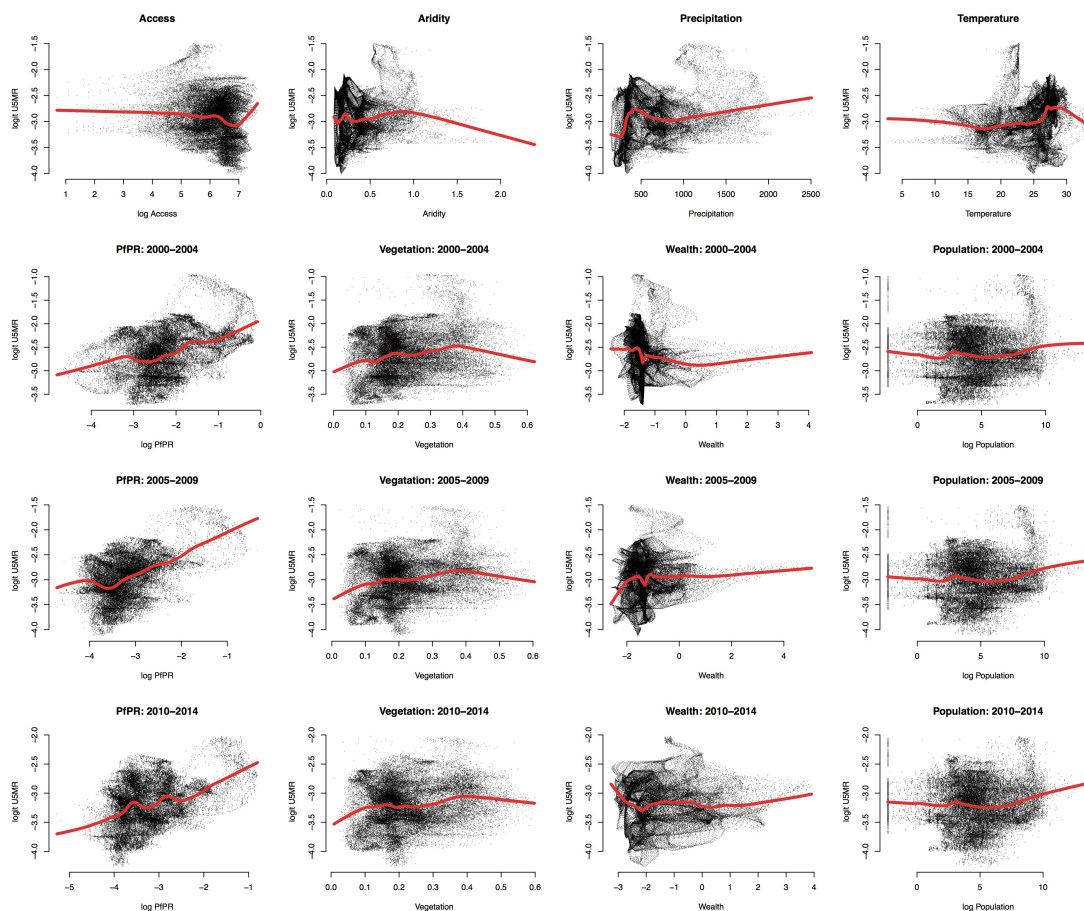


Figure 9. Scatterplots of the logit U5MR predictions versus the covariates, with a lowess smoother superimposed.

standard deviation compared to M_3 . A log-transformed version of the regional estimates under the four different models and the truth (test data) is in Figure 19.

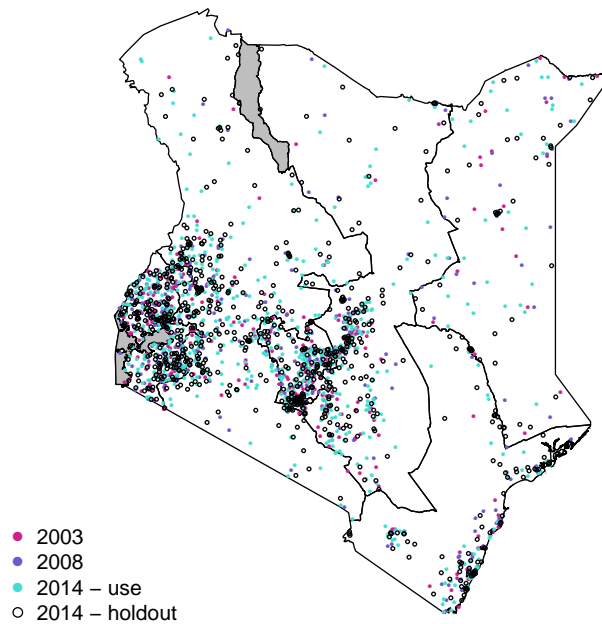


Figure 10. Cluster locations. All clusters in the 2003 and 2008 DHS and 785 clusters in the 2014 DHS were used as training data to build the covariate models.

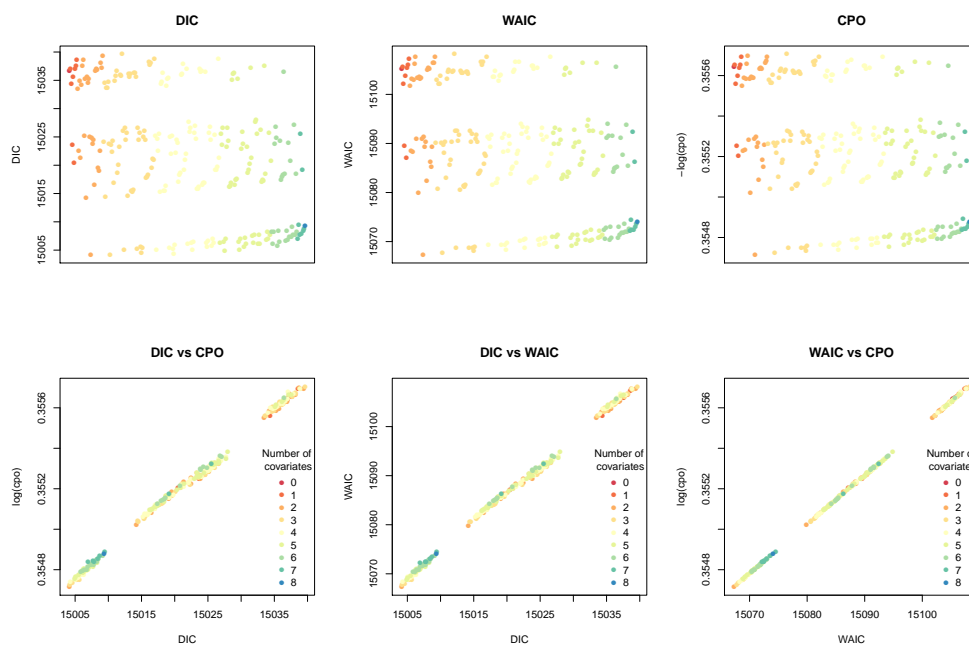


Figure 11. DIC, CPO and WAIC values for 256 possible covariate combinations for the model not involving a spatial random effect term. Colors indicate the number of covariates included in the model. The three “bands” observed is based on whether temperature and/or $P_f\text{PR}$ were included in the model.

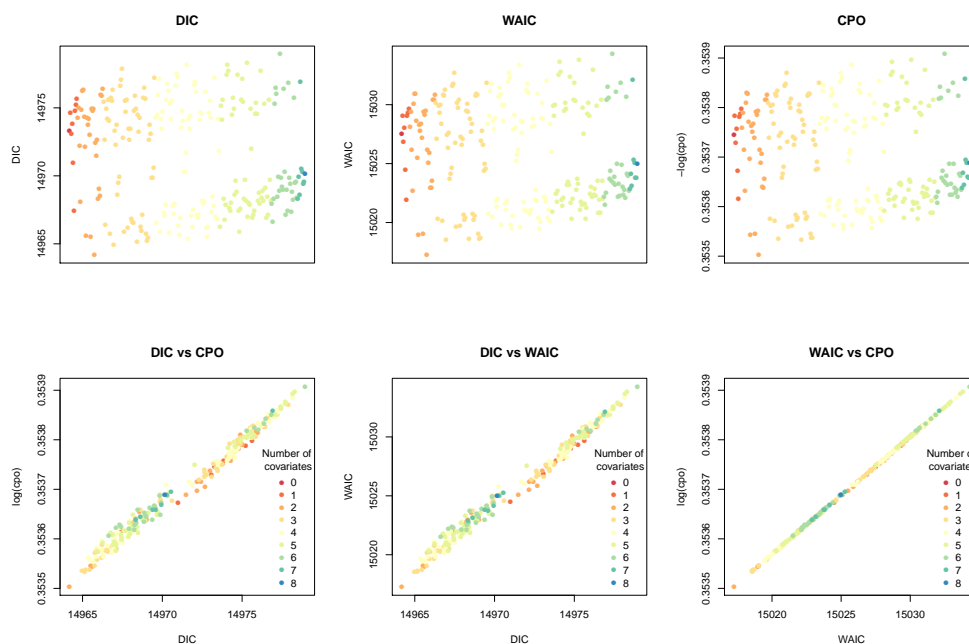


Figure 12. DIC, CPO and WAIC values for 256 possible covariate combinations for the model involving a spatial random effect term. Colors indicate the number of covariates included in the model. The best performing model across all measures had precipitation and *PfPR*. The worst performing model had all covariates except precipitation and malaria.

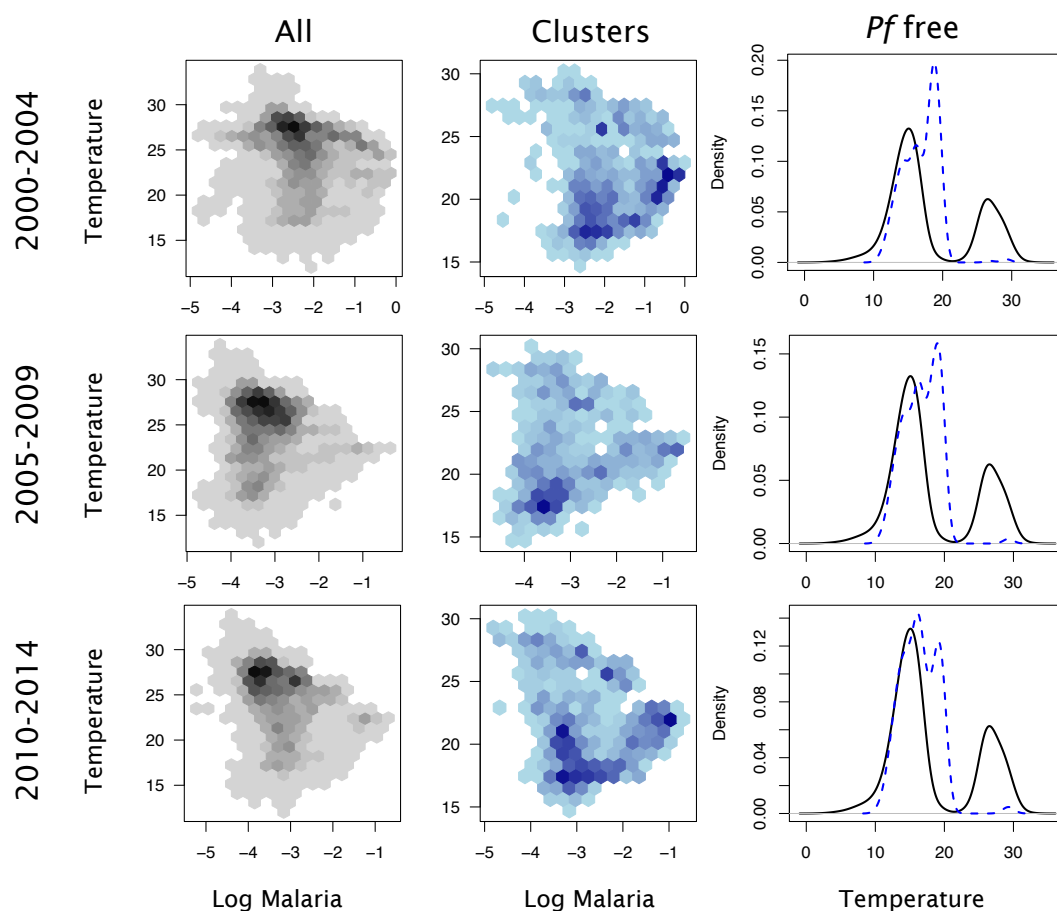


Figure 13. Bivariate plots showing the relationship between *PfPR* and temperature for each period. In blue, are the values at the cluster locations and black indicates the values over all of Kenya. Darker colors indicate more values.

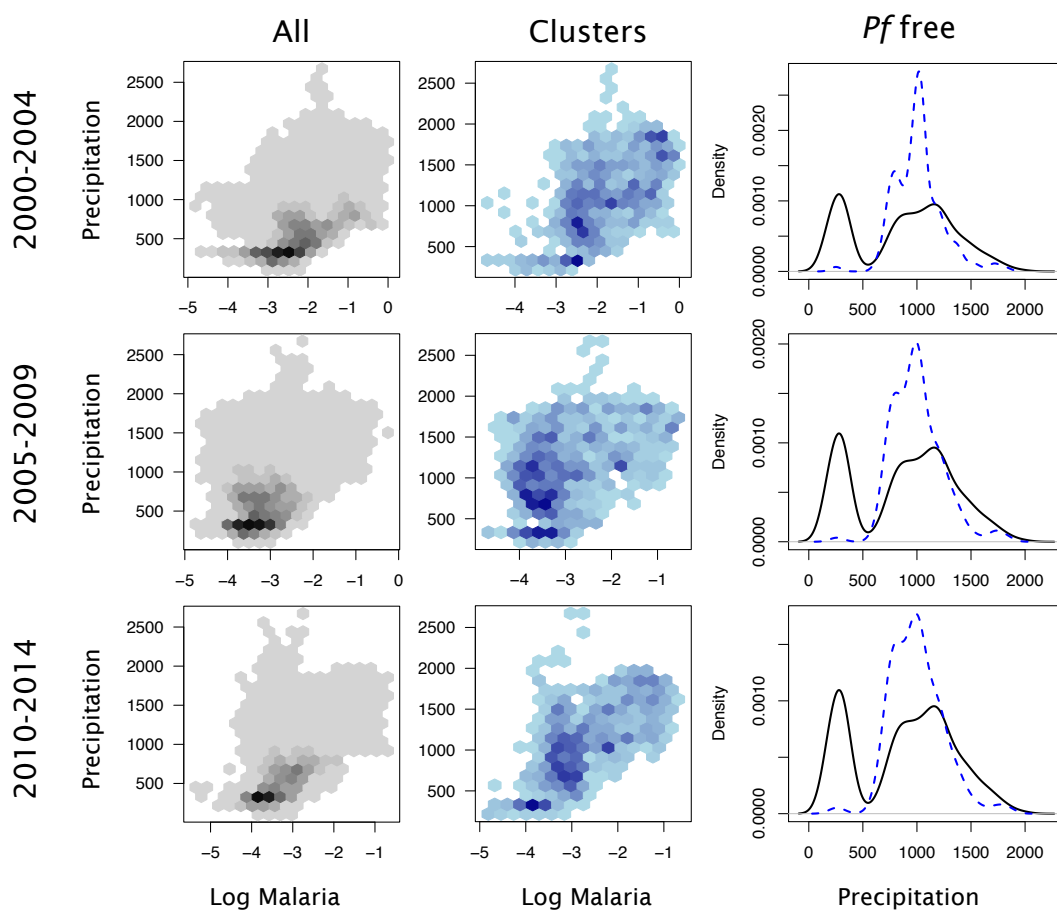


Figure 14. Bivariate plots showing the relationship between *Pf*PR and precipitation for each period. In blue, are the values at the cluster locations and black indicates the values over all of Kenya. Darker colors indicate more values.

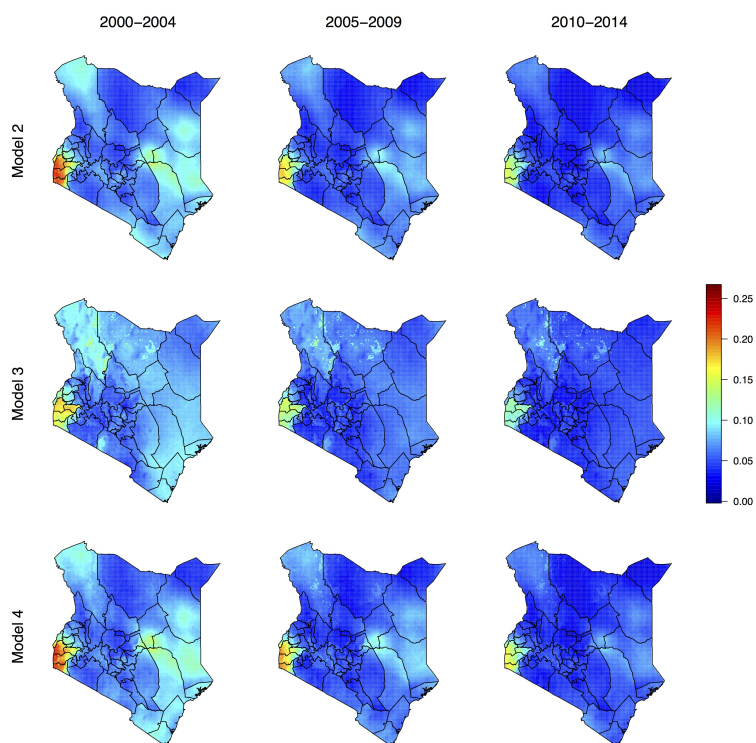


Figure 15. Predicted U5MR surface (posterior median) for M_2 , M_3 , and M_4 .

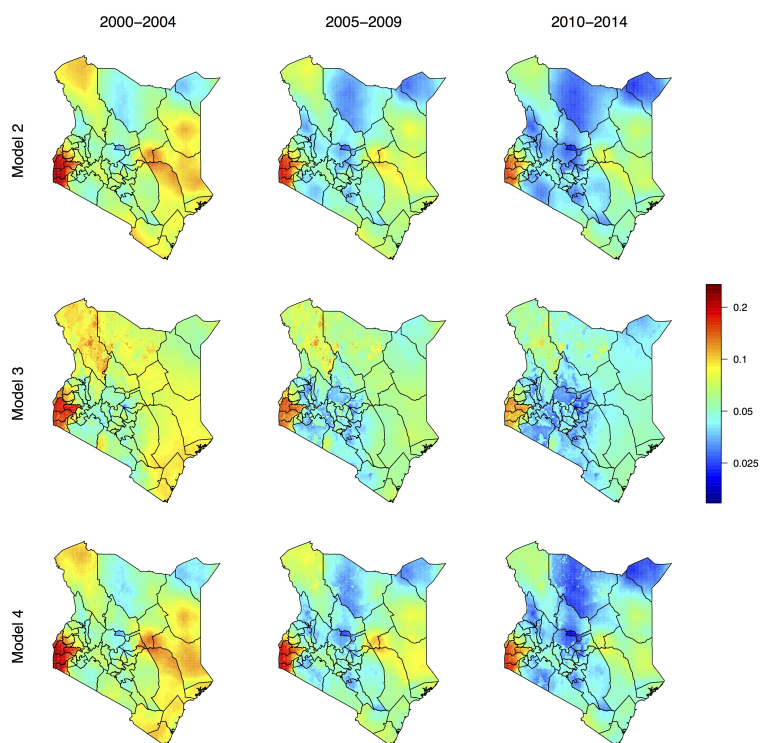


Figure 16. Predicted U5MR surface (posterior median) for M_2 , M_3 , and M_4 on log scale.

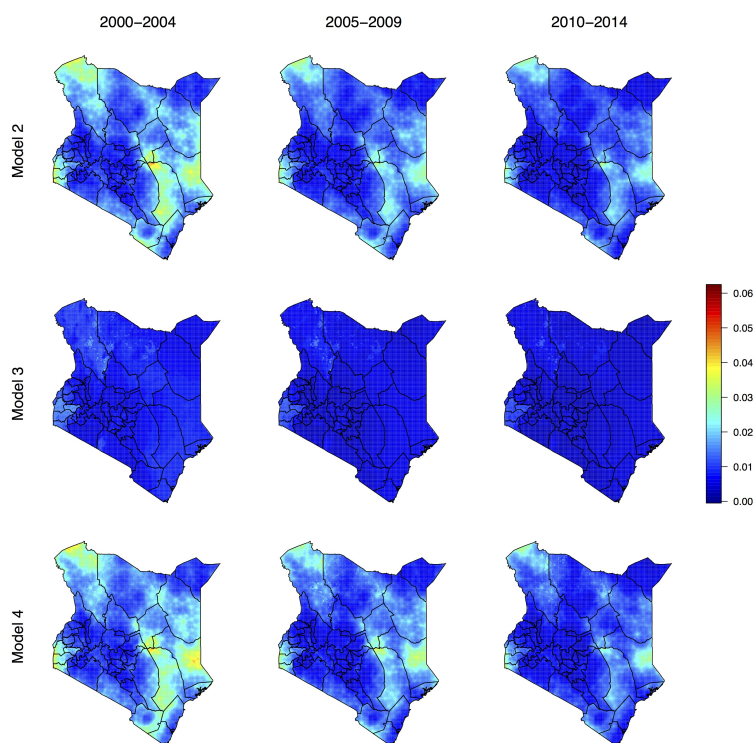


Figure 17. Posterior standard deviation for U5MR surface for M_2 , M_3 , and M_4 .

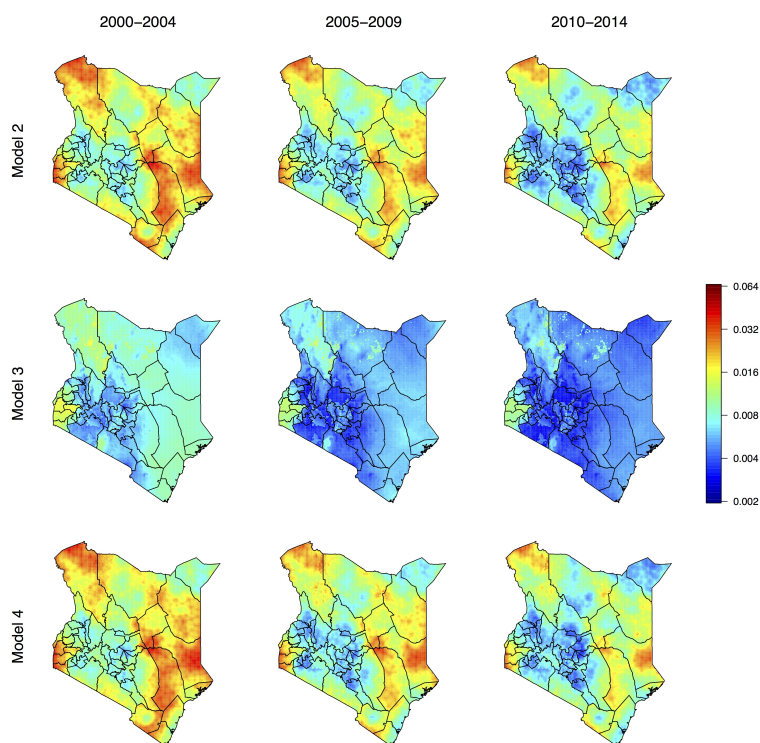


Figure 18. Posterior standard deviation for U5MR surface for M_2 , M_3 , and M_4 on log scale.

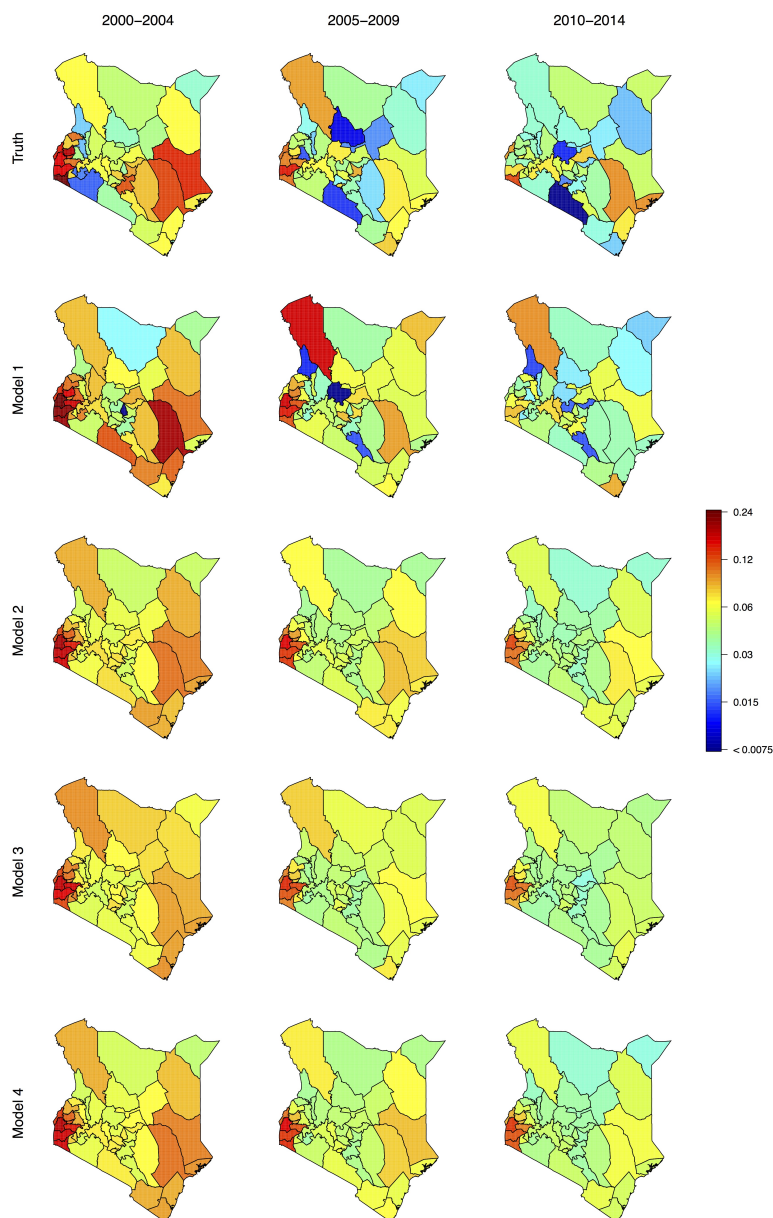


Figure 19. Regional predicted U5MR on log scale. Top row is the “truth”, i.e., direct estimates based on the 799 holdout locations in the 2014 survey. Model M_1 are the direct estimates based on the other clusters. Model M_2 is the spatial only model (no covariates). Model M_3 is the covariates only model (temperature and $PfPR$). Model M_4 is the spatial and covariates model (precipitation and $PfPR$).

We were also interested in whether and to what degree the coefficient values corresponding to the covariates of interest change by adding (or removing) a spatial random effect. These values are in Table 3. There was not much change between models that did not include the spatial random effect term (non-spatial) and models that did (spatial). Figure 20 visually depicts this; shown is the posterior median odds ratio (OR) surface.

Model	Temperature	Malaria: <i>Pf</i> free	Malaria: log <i>Pf</i> PR
Non-spatial	0.0630 (0.0413, 0.0845)	-0.192 (-0.490, 0.104)	0.186 (0.112, 0.259)
Spatial	0.0547 (0.0224, 0.0870)	-0.225 (-0.584, 0.136)	0.180 (0.0858, 0.272)
	Precipitation	Malaria: <i>Pf</i> free	Malaria: log <i>Pf</i> PR
Non-spatial	-0.261 (-0.419, -0.104)	-0.570 (-0.847, -0.295)	0.223 (0.150, 0.296)
Spatial	-0.295 (-0.529, -0.0668)	-0.402 (-0.752, -0.0481)	0.190 (0.0935, 0.284)

Table 3. Posterior medians and 95% credible intervals (CIs) for coefficients corresponding to covariates in different models. Non-spatial models refer to models that include the covariates, but not the spatial random effect. Spatial models refer to models that include covariates and the spatial random effect. Precipitation has been transformed to meters.

Figure 21 shows the predicted spatial random effect surface for M_2 and M_4 and summaries of the hyperparameters for the spatial random effect are in Table 4. There is not much difference between the two.

Parameter	M_2	M_4
λ (standard deviation)	0.441 (0.315, 0.630)	0.430 (0.305, 0.620)
ϕ (range)	1.81 (0.949, 3.72)	1.80 (0.939, 3.88)

Table 4. Posterior medians and 95% credible intervals (CIs) for hyperparameters of the spatial random effect in M_2 and M_4 .

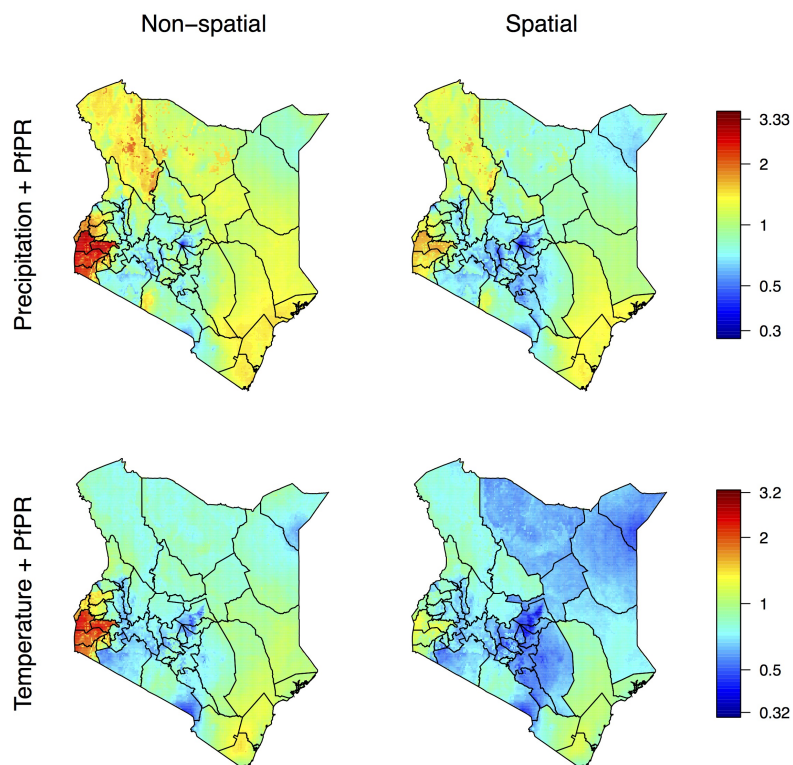


Figure 20. Surfaces depicting parameter estimates and how these values change with adding a spatial random effect. Plotted are the posterior median ORs comparing to a reference group. In the temperature and *PfPR* models, the reference group is the urban area of the Coast province, 20°C, and *Pf* free. In the precipitation and *PfPR* models, the reference group is the urban area of the Coast province, 500 mm of precipitation, and *Pf* free.

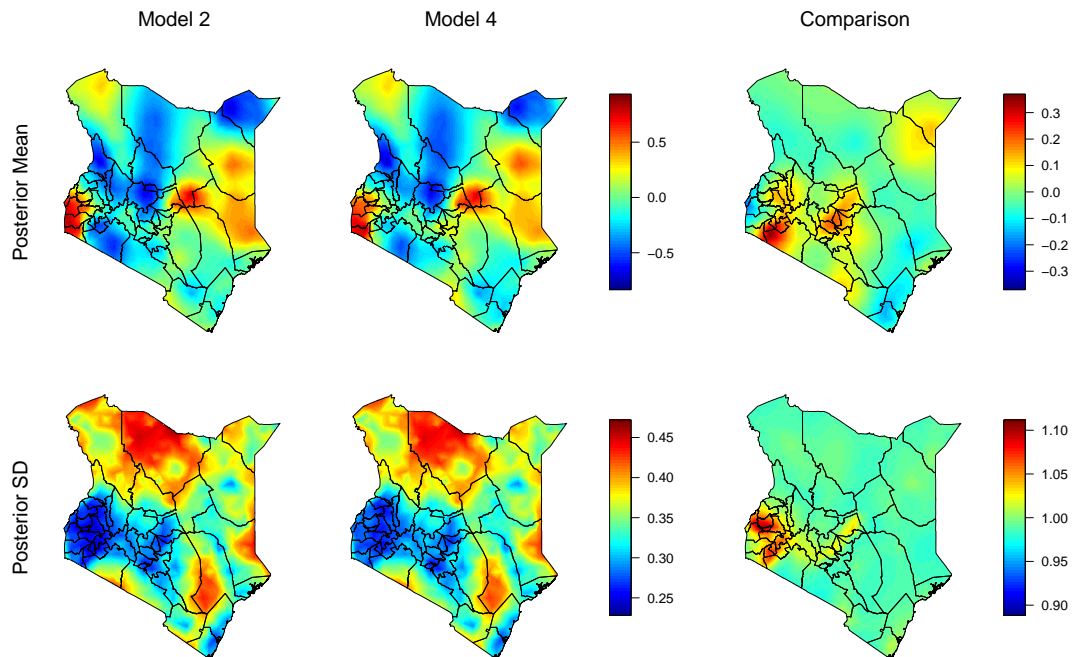


Figure 21. Latent spatial surface for Models 2 and 4. The last column is the comparison of the two models. For the posterior mean: spatial surface in Model 4 - spatial surface in Model 2. Thus, values greater than 0 indicate that the posterior mean of the spatial surface is higher under Model 4. For the posterior standard deviation: spatial surface in Model 4 divided by the spatial surface in Model 2. Thus, values greater than 1 indicate that the posterior standard deviation is greater in Model 4.

References

- Alkema, L. and J. New (2014). Global estimation of child mortality using a Bayesian B-spline bias-reduction model. *The Annals of Applied Statistics* 8, 2122–2149.
- Alkema, L., J. R. New, J. Pedersen, D. You, et al. (2014). Child mortality estimation 2013: an overview of updates in estimation methods by the United Nations Inter-Agency Group for Child Mortality Estimation. *PloS ONE* 9, e101112.
- Lindgren, F., H. Rue, and J. Linstrom (2011). An explicit link between Gaussian fields and Gaussian Markov random fields: the stochastic differential equation approach (with discussion). *Journal of the Royal Statistical Society, Series B* 73, 423–498.
- Rutstein, S. O. (2015). Steps to constructing the new DHS wealth index. Technical report, Rockville, MD.
- Rutstein, S. O. and K. Johnson (2004). *The DHS wealth index*. ORC Macro, MEASURE DHS.